EPJ D

Recognized by European Physical Society

Atomic, Molecular, Optical and Plasma Physics

Eur. Phys. J. D (2020) 74: 171 DOI: 10.1140/epjd/e2020-10079-6

Role of incoherent pumping field on control of optical bistability in a closed three-level ladder atomic system

Le Van Doai

edp sciences

Società Italiana di Fisica

Springer

Eur. Phys. J. D (2020) 74: 171
https://doi.org/10.1140/epjd/e2020-10079-6

THE EUROPEAN PHYSICAL JOURNAL D

Regular Article

Role of incoherent pumping field on control of optical bistability in a closed three-level ladder atomic system

Le Van Doai[a]

Vinh University, 182 Le Duan Street, Vinh City, Vietnam

Received 13 February 2020 / Received in final form 4 June 2020
Published online 20 August 2020

Abstract. In this paper, we analyze the role of incoherent pumping field on the control of optical bistability (OB) via the spontaneously generated coherence (SGC) and relative phase between laser fields in a closed three-level ladder-type atomic system. It is shown that in the presence of incoherent pumping field, the influences of the SGC and the relative phase of the OB behavior become more effective. Simultaneously, the threshold intensity and width of the OB reduce significantly when the incoherent pumping rate increases.

1 Introduction

As we have known optical bistability (OB) is an essential element in photonic devices such as optical transistors, optical memories, optical logic gates and optical switches, and so on [1]. Response speed and the sensitivity of the optical devices depend on the threshold intensity and width of the OB. Therefore, one is always looking for solutions to change the threshold intensity and the width of the OB, so that the operating characteristics of optical devices can be controlled. In recent years, the discovery of electromagnetically induced transparency (EIT) [2] has provided a simple solution to control the optical properties of the atomic medium including absorption and dispersion [3,4], Kerr nonlinearity [5–8], group velocity [9,10]. As a consequence, both the threshold intensity and width of the OB can be easily controlled and reduced significantly [11]. Initially, theoretical and experimental studies on the OB focused on three-level atomic systems including three-level Λ-, V- and ladder-type configurations [12–16]. It is found that the threshold intensity and width of the OB system are controlled by the intensity and frequency of laser fields. Recently, optical bistability in four- and five-level atomic systems has also been studied [17–19]. The studies have shown that the OB effect can occur at multiple frequency regions of the probe light.

In addition to the EIT effect, there is another kind of quantum interference arising from the spontaneous emission processes in atomic/molecular systems with nonorthogonality of electric dipole moments induced by coherent fields. Such interference creates an additional atomic coherence, usually called spontaneously generated coherence (SGC) [20] which modifies both transient and steady-state response of the medium. The influences of SGC on the optical properties of three-level atomic systems have been basically investigated for absorption and dispersion [21,22], group velocity [23,24], Kerr nonlinearity [25] and pulse propagation [26]. The effect of the SGC on OB behavior has also been analyzed in three-level Λ-type [27] and V-type [28] and ladder-type [29] systems. It is shown that the SGC can be used as a "knob" to manipulate the OB features.

Although the SGC can change atomic optical properties, the SGC effect is usually quite small due to the poor population in the upper excited state. In order to enhance this quantum interference effect, therefore, one introduces an incoherent pumping field to increase the population in the upper excited state and hence to increase the power of spontaneous emission processes in atomic/molecular systems. Indeed, in the presence of the pumping field, the influence of the SGC on absorption and dispersion [30,31], group velocity [32] and Kerr nonlinear effect [33] becomes more effective as incoherent pumping rate increases. Moreover, under the SGC with incoherent pumping, the optical responses of the atomic medium are very sensitive to the relative phase between the laser fields [30,31].

Up to now, the influences of SGC and incoherent pumping on optical bistability have been investigated in a closed three-level Λ-type [34], open three-level Λ-type [35], V-type [36] and open ladder-type [37] systems. However, the influences of the SGC and relative phase on the OB in a closed three-level ladder-type system in the presence of the incoherent pumping field have not been studied.

In order to bridge this gap, in this paper, we study the influence of incoherent pumping field on the control of optical bistability via the SGC and relative phase in a closed three-level ladder system. We find that in the presence of incoherent pumping field, the influences of the SGC and relative phase on the OB behavior become more sensitive. Moreover, the threshold intensity and width of the OB reduce effectively when the rate of incoherent pumping increases.

[a] e-mail: doailv@vinhuni.edu.vn

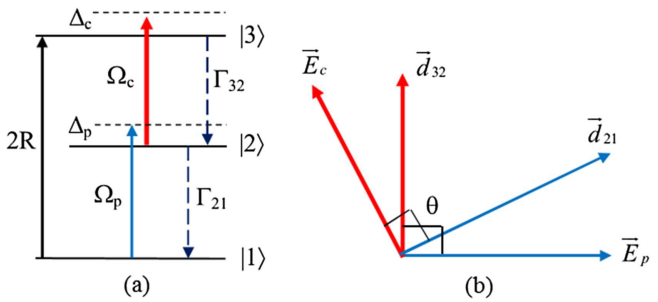

Fig. 1. (a) Schematic diagram of the closed three-level ladder-type atomic system. (b) The light polarizations are chosen so that only one field drives one transition.

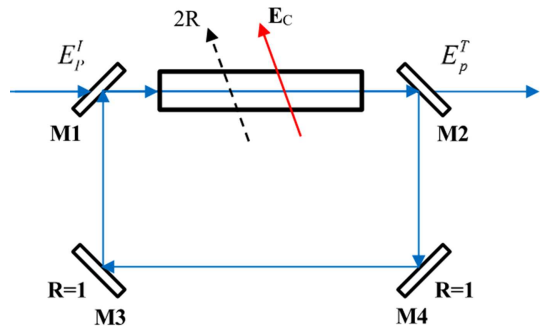

Fig. 2. Unidirectional ring cavity containing a three-level sample of length L: $E_{\rm p}^{I}$ and $E_{\rm p}^{T}$ are respectively the incident and transmitted probe fields while $E_{\rm c}$ and 2R are the coupling field and incoherent pumping that are not circulating inside the cavity.

2 Theoretical model

A closed three-level ladder-type atomic system interacting with two coherent fields is depicted in Figure 1a. In this scheme, a weak probe field with frequency $\omega_{\rm p}$ and amplitude $E_{\rm p}$ is used to drive the transition $|1\rangle \leftrightarrow |2\rangle$, while the transition $|2\rangle \leftrightarrow |3\rangle$ is driven by a strong coupling field with frequency $\omega_{\rm c}$ and amplitude $E_{\rm c}$. We denote Γ_{21} and Γ_{32} being the decay rate of the states $|2\rangle$ and $|3\rangle$, respectively. An incoherent pump with a pumping rate 2R is applied to the transition $|1\rangle \rightarrow |3\rangle$. The Rabi frequencies of the probe and coupling fields are respectively defined as $\Omega_{\rm p} = 2d_{21}E_{\rm p}/\hbar$ and $\Omega_{\rm c} = 2d_{32}E_{\rm c}/\hbar$, where d_{ij} is the electric dipole matrix element. To ensure that one field acts only one transition, we have chosen $\vec{E}_{\rm c}\perp\vec{d}_{21}$ and $\vec{E}_{\rm p}\perp\vec{d}_{32}$ as shown in Figure 1b.

Using the rotating-wave and the electric dipole approximations, we can write the density matrix equations of motion for this system as:

$$\dot{\rho}_{11} = -2R\rho_{11} + \Gamma_{21}\rho_{22} + \frac{i}{2}\Omega_{\rm p}\rho_{21} - \frac{i}{2}\Omega_{\rm p}\rho_{12}, \tag{1}$$

$$\dot{\rho}_{22} = -\Gamma_{21}\rho_{22} + \Gamma_{32}\rho_{33} + \frac{i}{2}\Omega_{\rm p}\rho_{12} - \frac{i}{2}\Omega_{\rm p}\rho_{21} + \frac{i}{2}\Omega_{\rm c}\rho_{32} - \frac{i}{2}\Omega_{\rm c}\rho_{23}, \tag{2}$$

$$\dot{\rho}_{33} = 2R\rho_{11} - \Gamma_{32}\rho_{33} - \frac{i}{2}\Omega_{\rm c}\rho_{32} + \frac{i}{2}\Omega_{\rm c}\rho_{23}, \tag{3}$$

$$\dot{\rho}_{21} = (i\Delta_{\rm p} + \gamma_{12} + R)\rho_{21} - \frac{i}{2}\Omega_{\rm p}(\rho_{22} - \rho_{11}) + \frac{i}{2}\Omega_{\rm c}\rho_{31} + 2p\sqrt{\Gamma_{12}\Gamma_{23}}\eta\rho_{32}, \tag{4}$$

$$\dot{\rho}_{32} = (i\Delta_{\rm c} - \gamma_{32})\,\rho_{32} - \frac{i}{2}\Omega_{\rm c}(\rho_{33} - \rho_{22}) - \frac{i}{2}\Omega_{\rm p}\rho_{31}, \tag{5}$$

$$\dot{\rho}_{31} = (i\Delta_{\rm p} + i\Delta_{\rm c} - \gamma_{31} - R)\,\rho_{31} - \frac{i}{2}\Omega_{\rm p}\rho_{32} + \frac{i}{2}\Omega_{\rm c}\rho_{21}. \tag{6}$$

Together with $\rho_{ij} = \rho_{ij}^{*}\ (i \neq j)$ and the conservation condition $\rho_{11}+\rho_{22}+\rho_{33} = 1$. In the above equations, γ_{ij} describes the coherence decay rate ρ_{ij} and generally given by:

$$\gamma_{ij} = \frac{1}{2}\left(\sum_{E_k<E_i}\Gamma_{ik} + \sum_{E_l<E_j}\Gamma_{lj}\right). \tag{7}$$

The detuning of the probe and coupling fields from their relevant atomic transitions are respectively defined by:

$$\Delta_{\rm p} = \omega_{\rm p} - \omega_{21}, \Delta_{\rm c} = \omega_{\rm c} - \omega_{32}. \tag{8}$$

The term $2p\sqrt{\gamma_{12}\gamma_{23}}\eta\rho_{23}$ describes the quantum interference effect resulting from the cross-coupling between the spontaneous emission paths $|1\rangle \leftrightarrow |2\rangle$ and $|2\rangle \leftrightarrow |3\rangle$ that represents the SGC effect, $p = \vec{d}_{21}\cdot\vec{d}_{32}/\left|\vec{d}_{21}\right|\left|\vec{d}_{32}\right| = \cos\theta$ with θ is the angles between the two dipole moments. It is obvious that when $\eta = 1$ the effect of SGC presents and the strength of the SGC will vary with θ; otherwise $\eta = 0$, the effect of the SGC is absent. Due to the SGC effect, the optical properties of the atomic system depend not only on the intensity and frequency but also on the phase of the probe and coupling fields, thus we have to treat Rabi frequencies as complex parameters. Let $\varphi_{\rm p}$ and $\varphi_{\rm c}$ are the phase of the probe and coupling fields, respectively, then we have $\Omega_{\rm p} = \Omega_1 e^{i\varphi_{\rm p}}$ and $\Omega_{\rm c} = \Omega_2 e^{i\varphi_{\rm c}}$, where Ω_1 and Ω_2 are real parameters. Let $\tilde{\rho}_{ii} = \rho_{ii}$, $\tilde{\rho}_{21} = \rho_{21}e^{-i\varphi_{\rm p}}$, $\tilde{\rho}_{32} = \rho_{32}e^{-i\varphi_{\rm c}}$, $\tilde{\rho}_{31} = \rho_{31}e^{-i(\varphi_{\rm p}+\varphi_{\rm c})}$, and from equations (1) to (6) we obtain:

$$\dot{\tilde{\rho}}_{11} = -2R\tilde{\rho}_{11} + \Gamma_{21}\tilde{\rho}_{22} + \frac{i}{2}\Omega_1\left(\tilde{\rho}_{21} - \tilde{\rho}_{12}\right), \tag{9}$$

$$\dot{\tilde{\rho}}_{22} = -\Gamma_{21}\tilde{\rho}_{22} + \Gamma_{32}\tilde{\rho}_{33} + \frac{i}{2}\Omega_1\left(\tilde{\rho}_{12} - \tilde{\rho}_{21}\right) + \frac{i}{2}\Omega_2\left(\tilde{\rho}_{32} - \tilde{\rho}_{23}\right), \tag{10}$$

$$\dot{\tilde{\rho}}_{33} = 2R\tilde{\rho}_{11} - \Gamma_{32}\tilde{\rho}_{33} - \frac{i}{2}\Omega_2\left(\tilde{\rho}_{32} - \tilde{\rho}_{23}\right), \tag{11}$$

$$\dot{\tilde{\rho}}_{21} = (i\Delta_{\rm p} - \gamma_{21} - R)\tilde{\rho}_{21} - \frac{i}{2}\Omega_1(\tilde{\rho}_{22} - \tilde{\rho}_{11}) + \frac{i}{2}\Omega_2\tilde{\rho}_{31} + 2p\sqrt{\Gamma_{12}\Gamma_{23}}\eta e^{i\varphi}\tilde{\rho}_{32}, \tag{12}$$

$$\dot{\tilde{\rho}}_{32} = (i\Delta_{\rm c} - \gamma_{32} - R)\,\tilde{\rho}_{32} - \frac{i}{2}\Omega_2(\tilde{\rho}_{33} - \tilde{\rho}_{22}) - \frac{i}{2}\Omega_1\tilde{\rho}_{31}, \tag{13}$$

$$\dot{\tilde{\rho}}_{31} = (i\Delta_{\rm p} + i\Delta_{\rm c} - \gamma_{31} - R)\,\tilde{\rho}_{31} - \frac{i}{2}\Omega_1\tilde{\rho}_{32} + \frac{i}{2}\Omega_2\tilde{\rho}_{21}, \tag{14}$$

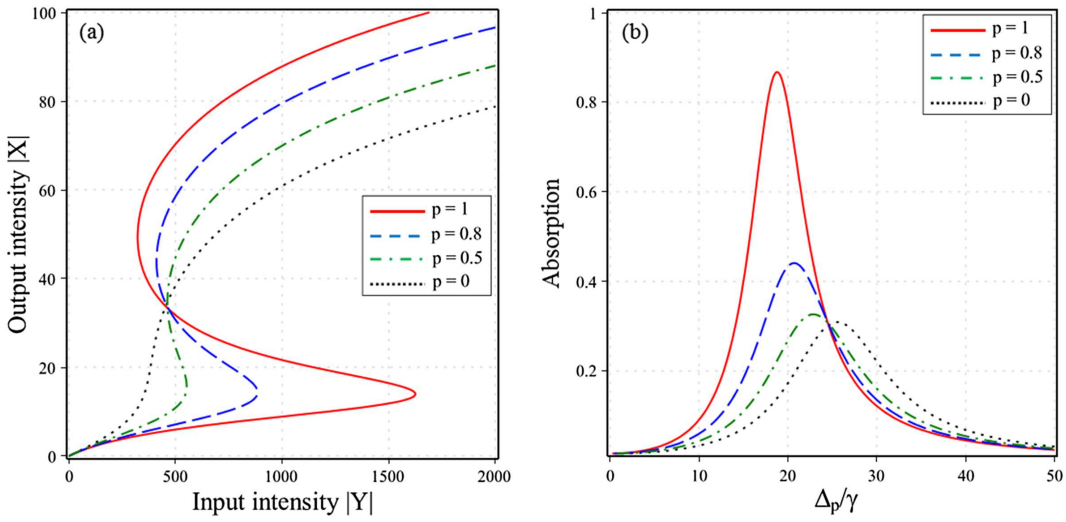

Fig. 3. (a) Plots of the input-output fields for different values of the strength of SGC when $R = 0$, $\varphi = 0$, $\Omega_2 = 50\gamma$, $\Delta_c = 0$, $\Delta_p = 20\gamma$ and $C = 2000\gamma$. (b) Variation of absorption (imaginary part of ρ_{21}) versus the probe frequency detuning with other parameters is similar to that in Figure 3a.

where $\varphi = \varphi_p - \varphi_c$ is the relative phase between the probe and the coupling fields.

Next, we put the atomic medium of length L composed of N three-level ladder systems in a unidirectional ring cavity (see Fig. 2). For simplicity, we assume that mirrors M3 and M4 have 100% reflectivity, whereas mirrors M1 and M2 are the same, each has a reflectivity R and transitivity T, with $R + T = 1$. In this ring cavity part of the probe field E_p is circulated in the cavity but nor the coupling field E_c.

The total electromagnetic field is

$$E = E_p e^{-i\omega_p t} + E_c e^{-i\omega_c t} + c.c. \tag{15}$$

Under the slowly varying envelop approximation, dynamic response of the medium for the probe field is governed by the wave propagation equation [19]:

$$\frac{\partial E_p}{\partial t} + c\frac{\partial E_p}{\partial z} = i\frac{\omega_p}{2\varepsilon_0}P(\omega_p), \tag{16}$$

where c and ε_0 are the speed of light and permittivity of free space, respectively; $P(\omega_p)$ is the slowly oscillating term of the induced polarization in transition $|2\rangle \leftrightarrow |1\rangle$ is given by:

$$P(\omega_p) = Nd_{21}\tilde{\rho}_{21}, \tag{17}$$

where d_{21} is the electric dipole moment, ρ_{21} is the corresponding density matrix element.

By substituting equation (17) into equation (16), we obtain the field amplitude under the steady-state:

$$\frac{\partial E_p}{\partial z} = i\frac{N\omega_p d_{21}}{2c\varepsilon_0}\tilde{\rho}_{21}. \tag{18}$$

For a single circulation of the probe field in the cavity, we denote probe field at the beginning and the end of the sample as $E_p(0)$ and $E_p(L)$, respectively (see Fig. 2). For a perfectly tuned cavity, the boundary conditions in the steady-state for the incident and transmitted probe fields are [19]:

$$E_p(L) = E_p^T/\sqrt{T}, \tag{19}$$

$$E_p(0) = \sqrt{T}E_p^I + RE_p(L). \tag{20}$$

The second term in the right-hand side of equation (20) describes the feedback from the mirror, which is an essential requirement for the generation of optical bistability. By normalizing the incident and transmitted probe field as

$$Y = \frac{d_{21}E_p^I}{\hbar\sqrt{T}}, \quad X = \frac{d_{21}E_p^T}{\hbar\sqrt{T}}, \tag{21}$$

we can get input-output intensity relationship for the probe field as

$$Y = X - iC\tilde{\rho}_{21}, \tag{22}$$

where

$$C = \frac{N\omega_p L d_{21}^2}{2c\varepsilon_0\hbar T}, \tag{23}$$

is the cooperation parameter of the atomic medium placed in the ring cavity.

3 Results and discussion

In order to find the steady-state solution of the output field intensity, we set the time derivatives $\dot{\tilde{\rho}}_{ij} = 0$ and solve numerically the corresponding density matrix equations together with the field equation (22). As an illustration, we apply to the case of ^{87}Rb atoms. In this case, the states $|1\rangle$, $|2\rangle$ and $|3\rangle$ are chosen as $5S_{1/2}(F = 1)$, $5P_{1/2}(F' = 2)$ and $5D_{3/2}(F'' = 2)$, respectively. The decay rates are [38]: $\Gamma_{21} = 6\,\text{MHz} = 6\gamma$, $\Gamma_{32} = 0.64\gamma$.

Firstly, we study the influence of the strength of SGC on the OB behavior in the absence of incoherent pumping by plotting the input-output fields versus parameter p when

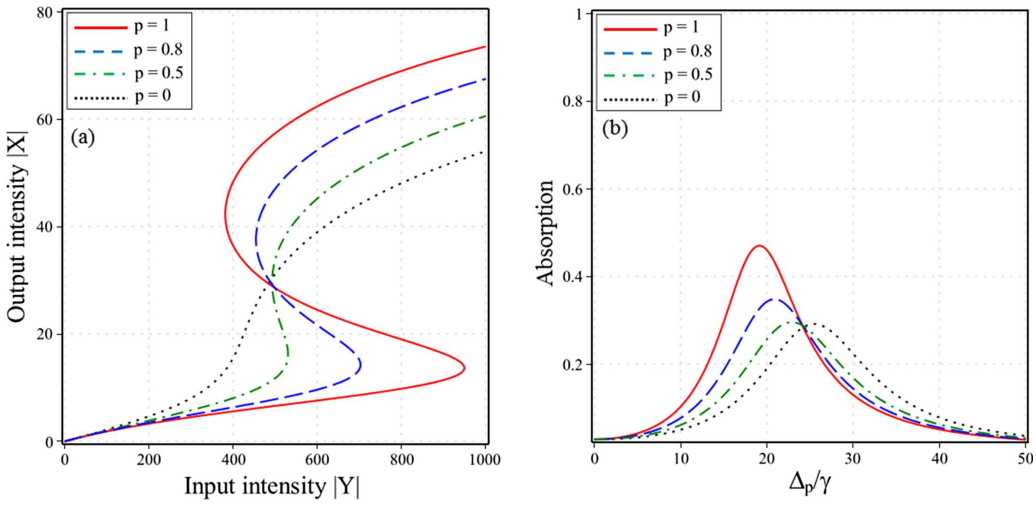

Fig. 4. (a) Plots of the input-output fields for different values of the strength of SGC when $R = 1$, $\varphi = 0$, $\Omega_2 = 50\gamma$, $\Delta_c = 0$, $\Delta_p = 20\gamma$ and $C = 2000\gamma$. (b) Variation of absorption versus the probe frequency detuning with other parameters is similar to that in Figure 4a.

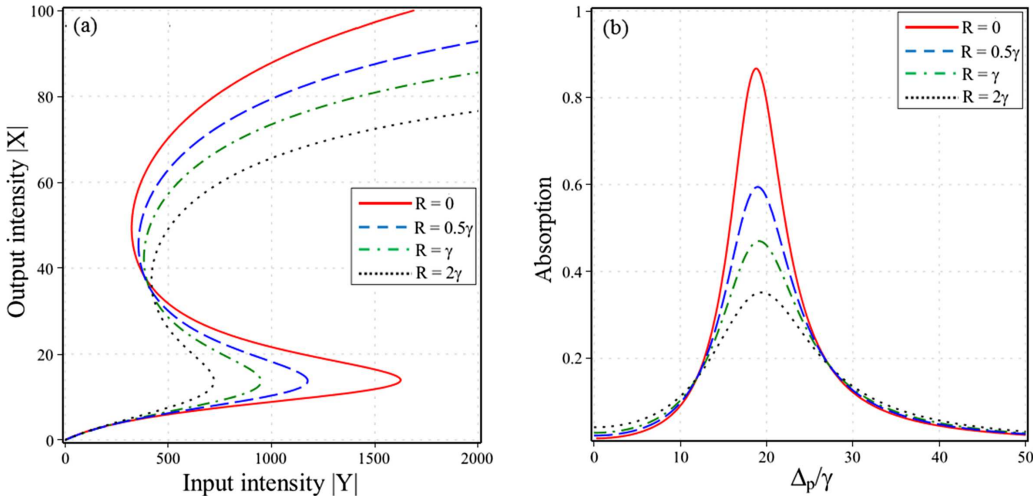

Fig. 5. (a) Plots of the input-output fields for different values of the incoherent pumping rate R when $p = 1$, $\varphi = 0$, $\Omega_2 = 50\gamma$, $\Delta_c = 0$, $\Delta_p = 20\gamma$ and $C = 2000\gamma$. (b) Variation of absorption versus the probe frequency detuning with other parameters is similar to that in Figure 5a.

the pumping rate $R = 0$ and the relative phase $\varphi = 0$, as shown in Figure 3a. Other parameters are employed in Figure 3a as $\Omega_2 = 50\gamma$, $\Delta_c = 20\gamma$, $\Delta_p = 0$ and $C = 2000\gamma$. It is seen clearly that for the given parameters, the OB behavior does not occur when $p = 0$ (without SGS), however, when $p = 0.5$ (with SGC) the OB has started to appear. Moreover, both the width and threshold intensity of OB increase with the growth of the parameter p. To explain this phenomenon, we plot the absorption coefficient versus parameter p as in Figure 3b. This figure shows that at $\Delta_p = 20\gamma$, the absorption coefficient is grown as the SGC increases, which leads to increasing the width and threshold intensity of the OB.

Now, we consider the impact of the incoherent pumping field on the SGC dependence of the OB by choosing the pumping rate $R = 1$ and investigating the influence of SGC on the OB behavior similar to Figure 3. The OB curves with respect to the strength of SGC for $R = 1$ are displayed in Figure 4a, while the plots of the corresponding absorption coefficient are described in Figure 4b. By comparing Figures 3a and 4a, we easily see that the presence of the incoherent pumping with $R = 1$ reduces significantly the width and threshold intensity of the OB. In addition, the OB behavior can be controlled with respect to the rate of incoherent pumping R as shown in Figure 5a. Here, we kept the strength of SGC at $p = 1$ and other parameters are similar to those in Figure 3. Figure 5a shows the width and threshold intensity of the OB decrease significantly when the rate of incoherent pumping increases. This may be different from the case of the open ladder-type system in which the bistable threshold can increase dramatically when the rate of incoherent pumping field is enhanced [37]. The phenomenon in Figure 5a can be explained based on the

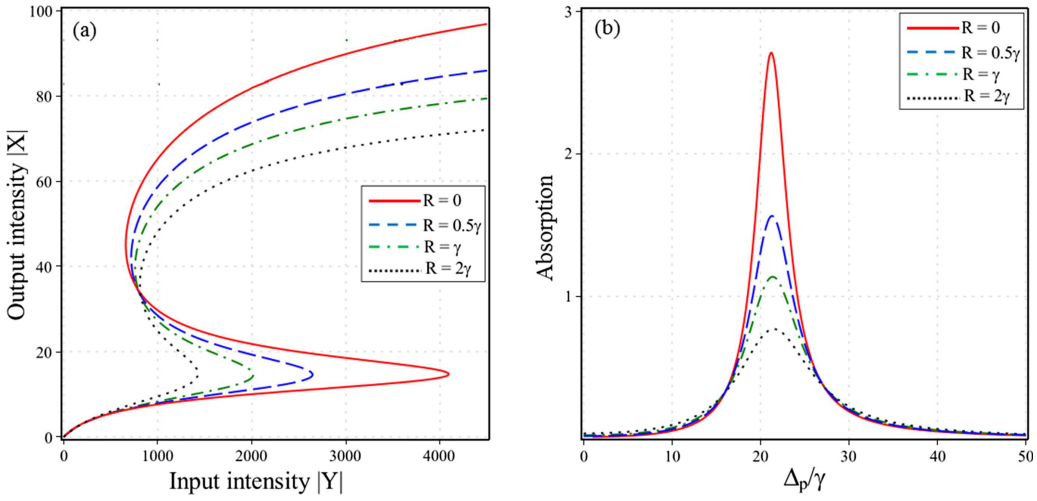

Fig. 6. (a) Plots of the input-output fields for different values of the incoherent pumping rate R when $p = 1$, $\varphi = \pi/4$, $\Omega_2 = 50\gamma$, $\Delta_c = 0$, $\Delta_p = 20\gamma$ and $C = 2000\gamma$. (b) Variation of absorption versus the probe frequency detuning with other parameters is similar to that in Figure 6a.

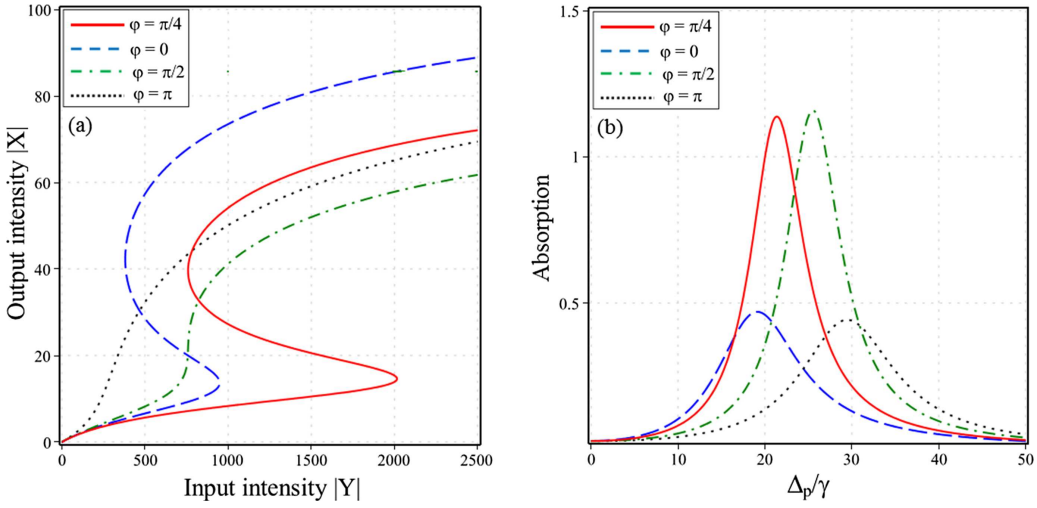

Fig. 7. (a) Plots of the input-output fields for different values of the relative phase φ when $p = 1$, $R = 1$, $\Omega_2 = 50\gamma$, $\Delta_c = 0$, $\Delta_p = 20\gamma$ and $C = 2000\gamma$. (b) Variation of absorption versus the probe frequency detuning with other parameters is similar to that in Figure 7a.

absorption spectrum that presented as in Figure 5b. It is clear that at $\Delta_p = 20\gamma$, the absorption reduces when the pumping rate increases, which can make the cavity field easier to reach saturation and therefore the threshold intensity decreases.

Next, we discuss the role of incoherent pumping in the relative phase dependence of the OB behavior. In Figure 6a, we plot the input-output fields for different values of the incoherent pumping rate R when $p = 1$ and the relative phase $\varphi = \pi/4$, while other parameters are chosen as in Figure 3. The investigation of Figure 6 demonstrates that the phase dependence of OB is very sensitive to the pumping rate. It shows clearly the width and threshold intensity of the OB decrease significantly when the rate of incoherent pumping R is enhanced. Physically, increasing the rate of incoherent pump field can reduce the probe absorption of the medium (see Fig. 6b at $\Delta_p = 20\gamma$) and hence decrease the width and threshold intensity of the OB. However, the comparison between Figures 5 and 6 shows that in the presence of the relative phase with $\varphi = \pi/4$ the OB thresholds become significantly larger than the case for $\varphi = 0$. On the other hand, under SGC condition, the OB behavior is also controlled according to the relative phase as shown in Figure 7a. The absorption spectrum for this case is presented in Figure 7b.

In Figure 8a, we plot the input-output fields for different values of the probe detuning Δ_p in the presence of incoherent pumping with $R = 1$ and the SGC with $p = 1$, while other parameters are chosen as in Figure 3. One can see that although at $\Delta_p = 0$ the absorption is zero (due to the EIT effect), but the nonlinear coefficient is also zero so the OB does not appear (see the dotted line in Fig. 8a). When the probe detuning Δ_p goes from $\Delta_p = 0$ to $\Delta_p = 20\gamma$ the probe absorption increases (see

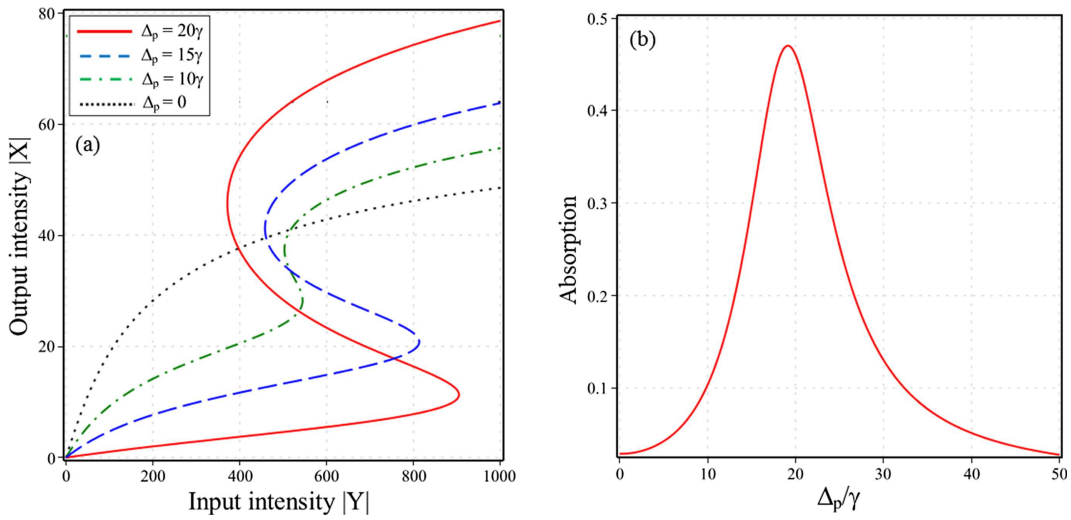

Fig. 8. (a) Plots of the input-output fields for different values of the frequency detuning Δ_p of the probe field when $\Omega_2 = 50\gamma$, $\Delta_c = 0$, $p = 1$, $R = 1$, $\varphi = 0$ and $C = 2000\gamma$. (b) Variation of absorption versus the probe frequency detuning with other parameters is similar to that in Figure 8a.

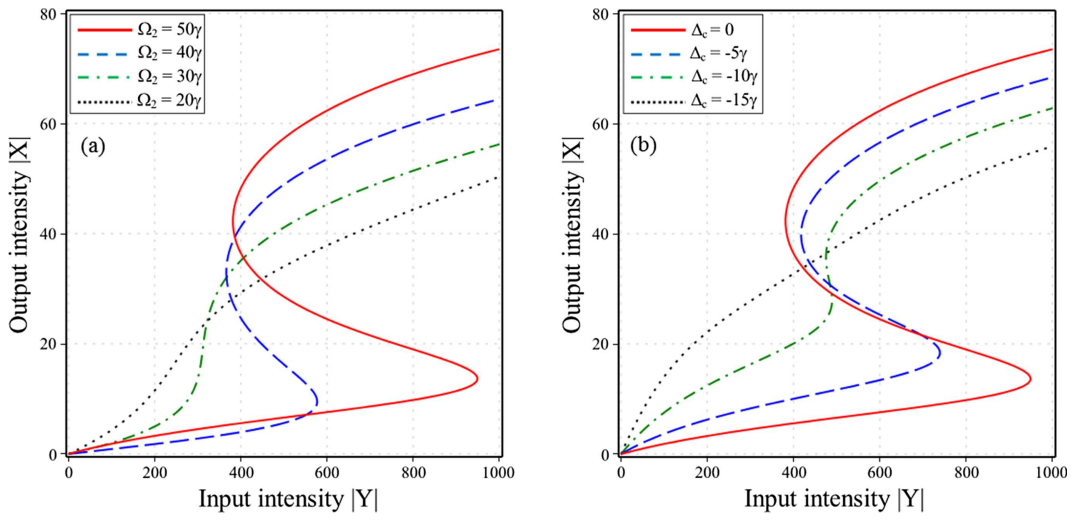

Fig. 9. Plots of the input-output fields for different values of the intensity Ω_2 (a) and frequency detuning Δ_c (b) of the coupling field when $\Delta_p = 20\gamma$, $p = 1$, $R = 1$, $\varphi = 0$, $C = 2000\gamma$, and $\Delta_c = 0$ for Figure 9a while $\Omega_2 = 50\gamma$ for Figure 9b.

Fig. 8b) and thus the width and threshold intensity of the OB increases.

Finally, we consider the influences of intensity and frequency of the coupling laser field on the OB behaviors as shown in Figures 9a and 9b, respectively. Here, the values of the strength of the SGC, the relative phase, and the pumping rate are chosen as $p = 1$, $\varphi = 0$ and $R = 1$. From these figures, one sees that the OB thresholds and width can be changed by adjusting the intensity or frequency detuning of the coupling field.

4 Conclusion

We have analyzed in detail the role of incoherent pumping field on the control of optical bistability with the spontaneously generated coherence and relative phase between applied fields in a closed three-level ladder-type atomic system. We found that the presence of the incoherent pumping field makes the influence of the SGC on OB behavior becomes more effective. The width and threshold intensity of the OB reduces significantly when the rate of incoherent pumping increases. This may be different from the case of the open ladder-type system in which the threshold intensity can increase dramatically when the rate of incoherent pumping field is enhanced. In addition, the phase dependence of OB is also very sensitive to the pumping rate. Therefore, the threshold intensity and width of OB can be effectively controlled with respect to the relative phase.

This work was supported by Vietnam's Ministry of Education and Training under Grant No. B2020-TDV-03.

Author contribution statement

The authors have equally contributed to the computations, analysis of the results and to the writing of the article.

References

1. E. Abraham, S.D. Smith, Rep. Prog. Phys. **45**, 815 (1982)
2. K.J. Boller, A. Imamoglu, S.E. Harris, Phys. Rev. Lett. **66**, 2593 (1991)
3. L.V. Doai, P.V. Trong, D.X. Khoa, N.H. Bang, Optik **125**, 3666 (2014)
4. D.X. Khoa, P.V. Trong, L.V. Doai, N.H. Bang, Phys. Scr. **91**, 035401 (2016)
5. D.X. Khoa, L.V. Doai, D.H. Son, N.H. Bang, J. Opt. Soc. Am. B **31**, 1330 (2014)
6. N.H. Bang, D.X. Khoa, D.H. Son, L.V. Doai, J. Opt. Soc. Am. B **36**, 3151 (2019)
7. L.V. Doai, N.L.T. An, D.X. Khoa, V.N. Sau, N.H. Bang, J. Opt. Soc. Am. B **36**, 2856 (2019)
8. L.V. Doai, J. Phys. B: At. Mol. Opt. Phys. **52**, 225501 (2019)
9. N.T. Anh, L.V. Doai, D.H. Son, N.H. Bang, Optik **171**, 721 (2018)
10. N.T. Anh, L.V. Doai, N.H. Bang, J. Opt. Soc. Am. B **35**, 1233 (2018)
11. N.H. Bang, L.V. Doai, D.X. Khoa, Commun. Phys. **28**, 1 (2019)
12. S.Q. Gong, S.D. Du, Z.Z. Xu, S.H. Pan, Phys. Lett. A **222**, 237 (1996)
13. H. Wang, D.J. Goorskey, M. Xiao, Phys. Rev. A **65**, 011801R (2001)
14. A. Joshi, A. Brown, H. Wang, M. Xiao, Phys. Rev. A **67**, 041801(R) (2003)
15. J. Li, Physica D **228**, 148 (2007)
16. Z. Wang, A.-X. Chen, Y. Bai, W.-X. Yang, R.-K. Lee, J. Opt. Soc. Am. B **29**, 2891 (2012)
17. H.R. Hamedi, S.H. Asadpour, M. Sahrai, B. Arzhang, D. Taherkhani, Opt. Quantum Electron. **45**, 295 (2013)
18. L. Ebrahimi Zohravi, R. Doostkam, S.M. Mousavi, M. Mahmoudi, Prog. Electromagn. Res. M **25**, 1 (2012)
19. D.X. Khoa, L.V. Doai, L.N.M. Anh, L.C. Trung, P.V. Thuan, N.T. Dung, N.H. Bang, J. Opt. Soc. Am. B **33**, 735 (2016)
20. J. Javanainen, Europhys. Lett. **17**, 407 (1992)
21. H.-M. Ma, S.-Q. Gong, Z.-R. Sun, R.-X. Li, Z.-Z. Xu, Chin. Phys. **11**, 2588 (2006)
22. M. Sahrai, Eur. Phys. J. Special Topics **160**, 383 (2008)
23. Y. Bai, H. Guo, D. Han, H. Sun, Phys. Lett. A **340**, 342 (2005)
24. N.H. Bang, L.N.M. Anh, N.T. Dung, L.V. Doai, Commun. Theor. Phys. **71**, 947 (2019)
25. Y.P. Niu, S.Q. Gong, Phys. Rev. A **73**, 053811 (2006)
26. H.M. Dong, L.V. Doai, N.H. Bang, Opt. Commun. **426**, 553 (2018)
27. A. Joshi, W. Yang, M. Xiao, Phys. Lett. A. **315**, 203 (2003)
28. A. Joshi, W. Yang, M. Xiao, Phys. Rev. A **68**, 015806 (2003)
29. D. Cheng, C. Liu, S. Gong, Phys. Lett. A **332**, 244 (2004)
30. A. Li, H. Ma, X. Tan, Y. Yang, D. Tong, X. Fan, Opt. Commun. **280**, 397 (2007)
31. X.J. Fan, A.Y. Li, F.G. Bu, H.X. Qiao, J. Du, Z.Z. Xu, Optik **119**, 540 (2008)
32. M. Mahmoudi, M. Sahrai, H. Tajalli, At. Mol. Opt. Phys. **39**, 1825 (2006)
33. A. Golestani, A. Darkhosh, H. Seifoory, A. Fali, A. Shams Shooli, Phys. Wave Phenom. **22**, 19 (2014)
34. H. Jafarzadeh, M. Sahrai, K. Jamshidi-Ghaleh, Appl. Phys. B **117**, 927 (2014)
35. Z. Wang, A.-X. Chen, Y. Bai, W.-X. Yang, R.-K. Lee, J. Opt. Soc. Am. B **29**, 2891 (2012)
36. M. Sahrai, S.H. Asadpour, R. Sadighi-Bonabi, J. Lumin. **131**, 2395 (2011)
37. S.H. Asadpour, H.R. Hamedi, H.R. Soleimani, J. Mod. Opt. **60**, 659 (2013)
38. Daniel Adam Steck, ^{87}Rb D Line Data: http://steck.us/alkalidata